



Cite this: *Chem. Soc. Rev.*, 2016,  
45, 1557

Received 3rd February 2015

DOI: 10.1039/c5cs00105f

[www.rsc.org/chemscrev](http://www.rsc.org/chemscrev)

## Cascade polycyclizations in natural product synthesis

R. Ardkhean, D. F. J. Caputo, S. M. Morrow, H. Shi, Y. Xiong and E. A. Anderson\*

Cascade (domino) reactions have an unparalleled ability to generate molecular complexity from relatively simple starting materials; these transformations are particularly appealing when multiple rings are forged during this process. In this tutorial review, we cover recent highlights in cascade polycyclizations as applied to natural product synthesis, including pericyclic, heteroatom-mediated, cationic, metal-catalyzed, organocatalytic, and radical sequences.

### Key learning points

- (1) Cascade (domino) polycyclizations are among the most efficient, ambitious, and elegant tools for the synthesis of polycyclic natural products.
- (2) A variety of reaction types (pericyclic, heteroatom-mediated, cationic, metal-catalyzed, organocatalytic and radical) can be employed in cascade polycyclizations.
- (3) Cascade reactions can lead to new biosynthetic hypotheses, highlighted in this review through homo- and heterochiral dimerizations.
- (4) Important advances have been made in enantioselective polyene cyclizations promoted by transition metal catalysts and halonium ions.
- (5) Transition metal-catalyzed cascades offer efficient and unique methods for bond formation to prepare polycyclic natural products.

## Introduction

Natural product total synthesis represents a pinnacle of achievement and ambition in organic chemistry, and is arguably fundamental to the successful commercial development of natural products or their derivatives as bioactive agents.<sup>1–3</sup> Not least due to the advent of new catalytic processes (such as C–H activation, organocatalysis, and photoredox chemistry, amongst others), combined with the evergreen creativity of the synthetic organic chemist, can truly concise and efficient routes to complex bioactive natural products be realized. Chief among the armaments of the modern synthetic practitioner are cascade (domino) reactions – transformations that by their very nature not only achieve significant increases in molecular complexity and reductions in overall step count, but also demonstrate synthetic elegance and creativity.<sup>4</sup> In this review, we highlight achievements at the frontier of this field, where cascade reactions are deployed to prepare polycyclic frameworks, embedded in the setting of complex molecule synthesis. As in the style of a previous coverage,<sup>5</sup> these domino processes are loosely divided into themes of pericyclic, heteroatom-mediated,

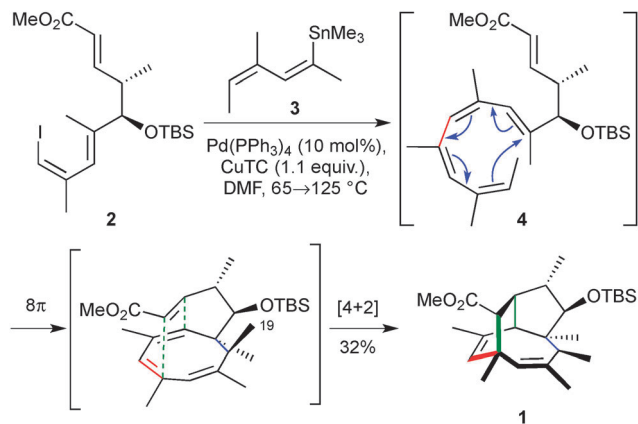
cationic, metal-catalyzed, organocatalytic, and radical cascades. The aim of this review is therefore not to provide a comprehensive coverage,<sup>6</sup> but to present the reader with a flavour of the state of the art, as well as to describe impressive new developments and technologies in each of these themes.

## Pericyclic cascades

Much continues to be learnt from Nature's use of pericyclic cascades to assemble complex natural product frameworks, and synthetic chemists have long recognized that biomimetic cascades<sup>7</sup> enable powerful retrosynthetic disconnections, with electrocyclic components commonplace in these sequences.<sup>8</sup> The Trauner group's synthesis of the core ring structure (**1**, Scheme 1) of (–)-PF-1018,<sup>9</sup> a tricyclic insecticide isolated from *Humicola* sp., is notable for its unusual Diels–Alder termination step following a tetraene 8π-electrocyclization, rather than the 6π-electrocyclization usually observed with monocyclic cyclooctatrienes.<sup>8</sup> The cascade is triggered by Stille coupling of vinyl iodide **2** with vinyl stannane **3** to generate tetraene **4**. 8π-Electrocyclization and subsequent intramolecular Diels–Alder (IMDA) cycloaddition delivered tricycle **1** in 32% yield as a single diastereomer. This reflects strong torquoselectivity (*i.e.*, the rotational directionality of the conrotatory

Chemistry Research Laboratory, 12 Mansfield Road, Oxford, OX1 3TA, UK.  
E-mail: [edward.anderson@chem.ox.ac.uk](mailto:edward.anderson@chem.ox.ac.uk); Fax: +44 (0)1865 285002;  
Tel: +44 (0)1865 285000

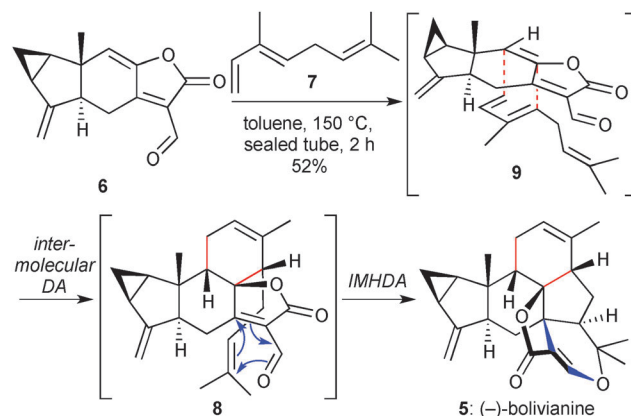




**Scheme 1** Stille/8 $\pi$ /IMDA cascade towards PF-1018 (Trauner and co-workers).

cyclization), arising from a specific helical arrangement of the cyclizing tetraene. The avoidance of the competing 6 $\pi$  reaction may in part be due to the high degree of torsional strain that might arise between the C19 methyl and enoate sidechain in the required planar arrangement of the 8-membered ring.

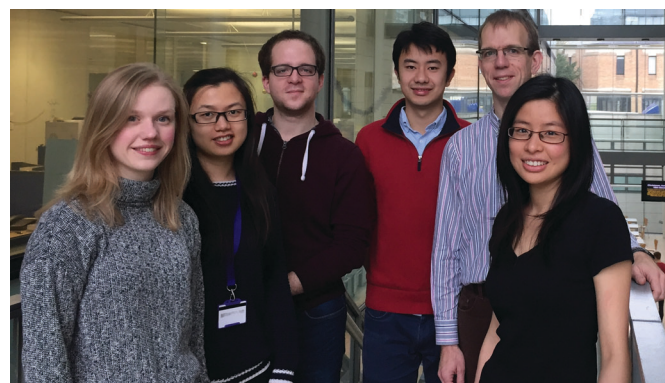
A remarkable intermolecular/intramolecular Diels–Alder cascade has been realized in the Liu group's bioinspired 14 step synthesis of (–)-bolivianine (5, Scheme 2),<sup>10,11</sup> the heptacyclic skeleton and nine contiguous stereocentres of which pose a significant and attractive synthetic proposition. The final step of this synthesis is the reaction of onoseriolide aldehyde 6 (itself thought to be an important intermediate in the biosynthesis of bolivianine) with  $\beta$ -(E)-ocimene (7, a compound again detected in the producing plant, *Hedyosmum angustifolium*). These two components undergo a Diels–Alder/intramolecular hetero-Diels–Alder cascade *via* intermediate 8 to give the natural product in 52% yield as a single diastereomer. This selectivity is rationalized by an *endo*-selective cycloaddition of the diene on the bottom face of the onoseriolide framework (9). Although the first step of this cascade



**Scheme 2** Biomimetic cycloaddition cascade in the synthesis of (–)-bolivianine (Liu and co-workers).

required elevated temperatures and the presence of the sidechain aldehyde to activate the dienophile, it is notable that the second Diels–Alder process was found to occur spontaneously at room temperature, adding support to the possibility that this synthesis indeed resembles the biosynthetic pathway. This work is particularly impressive given the challenge posed by an intermolecular cycloaddition initiation step.

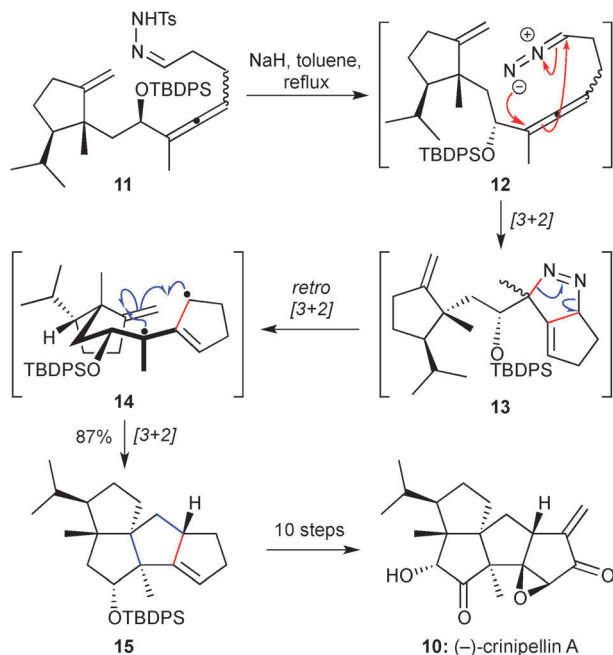
Non-biomimetic pericyclic cascades also offer excellent synthetic opportunities. In this context, an elegant polycyclization featuring two unusual cycloadditions has been developed by the Lee group in a landmark total synthesis of (–)-crinipellin A (10, Scheme 3).<sup>12</sup> The key cycloaddition sequence is initiated by treatment of hydrazone 11 with sodium hydride, which promotes formation of diazo compound 12. A spontaneous [3+2] cycloaddition of 12 with the pendent allene leads to diazene intermediate 13 (as an inconsequential mixture of diastereomers), extrusion of nitrogen from which gives trimethylenemethane diyl 14. Despite high steric congestion, a further [3+2] cycloaddition of this intermediate gives tetraquinane 15 in an outstanding 87%



From left to right: Morrow, Xiong, Caputo, Shi, Anderson, Ardkhean

Ed Anderson took up an EPSRC Advanced Research Fellowship at Oxford in 2007, and was appointed as an Associate Professor at Jesus College, Oxford in 2009. His research interests encompass a wide range of synthetic organic chemistry, and include transition metal catalysis, organosilicon chemistry, cascade reactions, and their applications in synthesis.





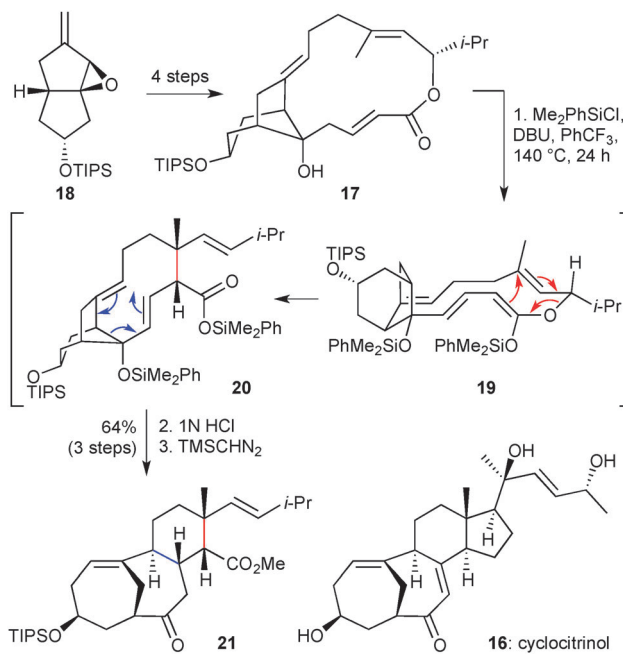
**Scheme 3** [3+2] cycloaddition cascade, *via* a trimethylenemethane diyl, in the synthesis of (–)-crinipellin A (Lee and co-workers).

yield as a single diastereomer; a pseudo-equatorial positioning of substituents likely controls this stereochemical outcome. This creative step forges the crinipellin skeleton and sets three stereocentres, including two contiguous quaternary carbon atoms.

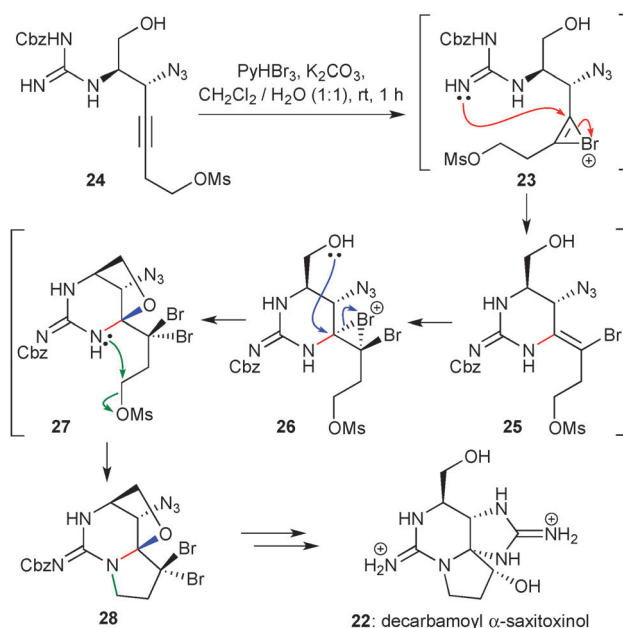
A final ‘pericyclic’ example is found in Leighton and co-workers’ expedient route to the steroidal core of cyclocitrinol (**16**, Scheme 4).<sup>13</sup> The central challenge in the construction of this polycyclic skeleton lies with the strained [4.4.1]-bicycle that features a bridgehead double bond. The group identified an Ireland–Claisen/Cope rearrangement ring contraction strategy as a possible means to access this challenging structure.<sup>14</sup> To test this, macrolactone **17** was efficiently synthesized in just 4 steps from **18**, *via* a twofold alkene metathesis. Treatment of **17** with chlorodimethylphenylsilane and DBU then gives silyl enol ether **19**. Through the illustrated boat conformation, Ireland–Claisen rearrangement of **19** affords **20**, which then undergoes a strain-relieving Cope rearrangement to give the tricyclic product **21**. The presence of an isopropyl group on the lactone ring is crucial to avoid side reactions; through this sequence, a 64% yield of **21** is obtained after hydrolysis and esterification.

## Heteroatom-mediated cascades

Heteroatoms continue to offer an excellent means to promote cascade polycyclizations in natural product synthesis, and four examples have been selected that illustrate recent developments in this field. Firstly, a novel double bromocyclization has been employed by Sawayama and Nishikawa to establish the cyclic guanidine–pyrrolidine structure found in decarbamoyl  $\alpha$ -saxitoxinol (**22**, Scheme 5), a non-toxic analogue of saxitoxin produced by the cyanobacterium *Lyngbya wollei*.<sup>15</sup> In a biphasic medium of

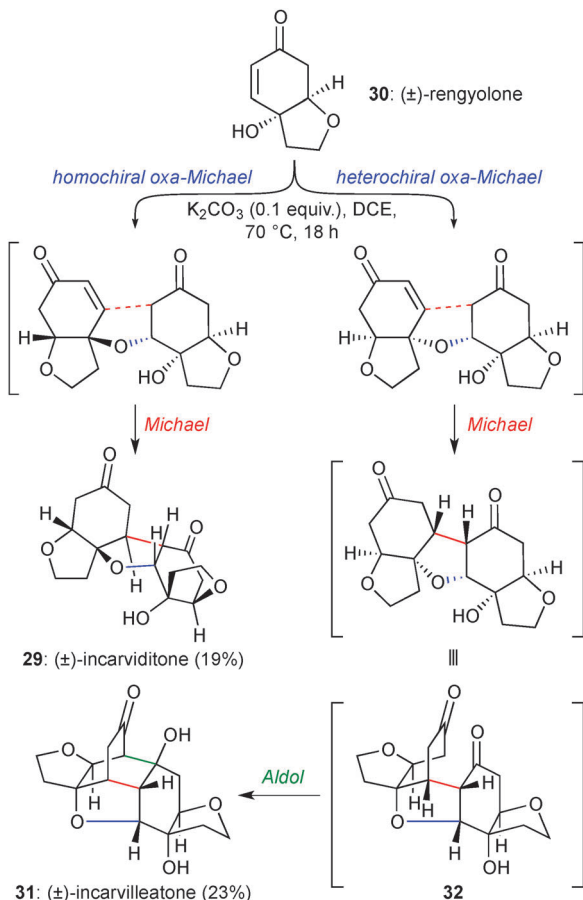


**Scheme 4** Cascade pericyclic ring contraction route to the core of cyclocitrinol (Leighton and co-workers).



**Scheme 5** Double-bromocyclization approach to decarbamoyl  $\alpha$ -saxitoxinol (Sawayama and Nishikawa).

water/dichloromethane, a stereospecific cascade cyclization is initiated by generation of a bromonium ion **23** upon treatment of alkyne **24** with pyridinium tribromide. This highly reactive intermediate undergoes intramolecular nucleophilic displacement by the guanidine residue, leading to enamine **25**. Formation of a bromonium ion **26** from this enamine then promotes the construction of the bridging oxacycle, giving spiroaminal ether intermediate **27**. Finally, an intramolecular *N*-alkylation concludes



Scheme 6 Homochiral and heterochiral oxa-Michael initiated cascades to  $(\pm)$ -incarviditone and  $(\pm)$ -incarvilleatone (Lawrence and co-workers).

the cascade cyclization to afford the tricyclic skeleton 28. Although the oxacyclic ring is eventually opened, this aminal ether later facilitates construction of the second guanidine ring in the natural product.

Domino biomimetic sequences can often lead to serendipitous discoveries. The first total synthesis of  $(\pm)$ -incarviditone (29, Scheme 6), reported by Lawrence and co-workers,<sup>16</sup> exploits an elegant biomimetic heteroatom-mediated cascade in which the racemic natural product  $(\pm)$ -rengyolone 30 undergoes homochiral dimerization *via* an oxa-Michael/Michael addition to afford 29. However, formed in equal quantity in this reaction is product 31, which arises from a separate three-step cascade beginning with a heterochiral dimerization of  $(\pm)$ -rengyolone – a pathway that is entirely reasonable given a racemic starting material. Here, the conformation of Michael adduct 32 is such that a further aldol cyclization is possible (leading to 31). In fact, this compound itself turned out to be a natural product (incarvilleatone) whose existence was disclosed only during the preparation of the synthetic manuscript. Thus, depending on the combination of two equivalent, or different enantiomers of rengyolone (30), different natural product structures are accessed – a fascinating phenomenon that we will return to later in this review.

Heteroatom-mediated epoxide ring-opening cascades are an ideal biomimetic tactic for the synthesis of poly-oxacyclic

natural products.<sup>17–19</sup> Although it is generally recognized in these reactions that *exo* ring-opening (*via* a ‘spiro’ transition state) is usually kinetically favoured over *endo* ring-opening (*via* a ‘fused’ transition state), much synthetic effort has been directed towards controlling this regioselectivity problem. Two examples are presented here that offer new solutions through the innovative generation of epoxonium ions; the challenge faced with such chemistry is the selective activation of the desired epoxide in a polyepoxide substrate, which can be problematic when ‘traditional’ Lewis acids are employed.

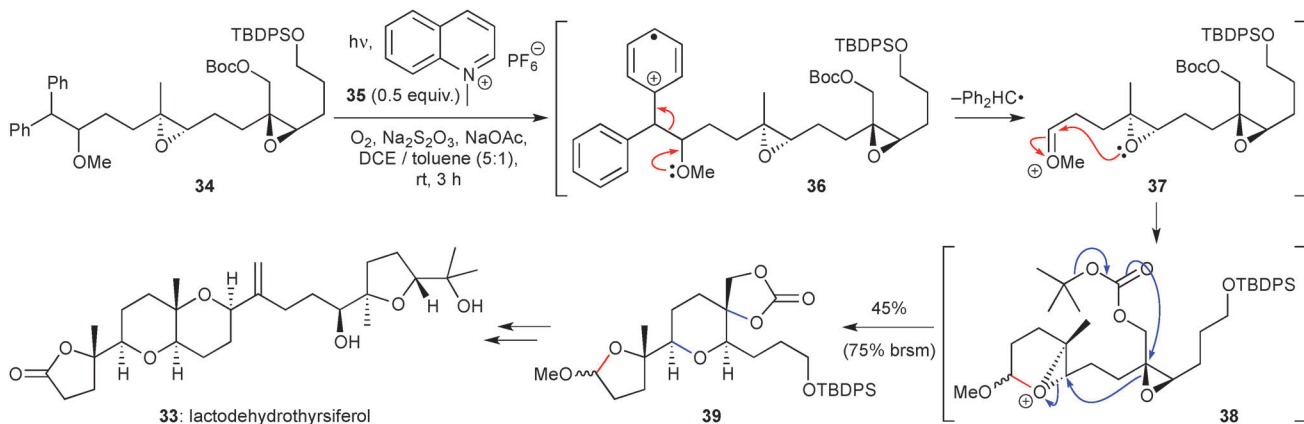
The first example is a total synthesis of the protein phosphatase 2A inhibitor lactodehydrothysiferol (33, Scheme 7), reported by the Floreancig group.<sup>20</sup> The key regioselective epoxonium ion-generating transformation involves a photochemically-mediated oxidation of a homobenzhydrol ether.<sup>21</sup> The reaction initiates with 34, which through single electron transfer to the excited state of quinolinium cation 35 generates intermediate radical cation 36.<sup>22</sup> This spontaneously loses a benzhydrol radical, leading to oxocarbenium ion 37, attack onto which by the proximal epoxide gives epoxonium ion 38. This in turn undergoes a double cyclization cascade with the next epoxide and the *tert*-butoxycarbonate (with concomitant loss of a *tert*-butyl cation), to afford tricycle 39.

Teurilene (40, Scheme 8) is a cytotoxic triterpene polyether biosynthetically linked to the thysiferol family. Martin and co-workers have developed a mild cascade route to the teurilene oxatricyclic ring system<sup>23</sup> that employs a Nicholas reaction.<sup>24</sup> Thus, exposure of the dicobalt hexacarbonyl-complexed propargylic alcohol 41 to silica gel in dichloromethane at room temperature provides a sufficiently acidic reaction medium to promote ionization, epoxonium ion formation (42), and cascade cyclization of the tris-epoxide. Oxidative liberation of the alkyne by CAN-mediated cobalt decomplexation afforded tris-tetrahydrofuran 43 in 75% yield. The formation of an epimeric mixture at the propargylic position was not problematic, as an isomerization later established the desired configuration. Interestingly, and contrary to the lactodehydrothysiferol example, the authors did not observe an additional cyclization of the Boc group onto the intermediate cation.

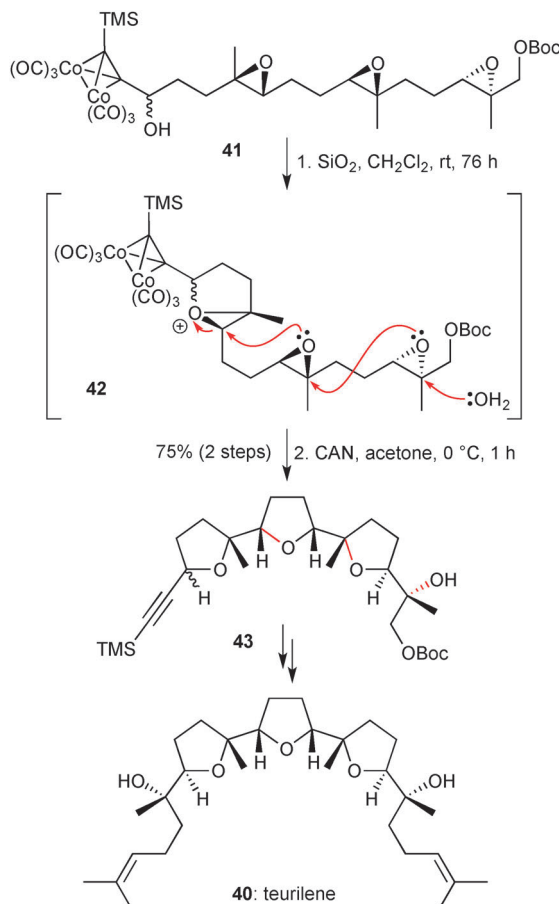
## Cationic cascades

Cation-induced polyene cyclizations offer a powerful means to construct complex polycyclic structures *via* multiple carbon–carbon bond formations. Such pathways are well known in Nature; however, controlling the regio- and stereochemistry of these processes in a synthetic context is highly challenging. A landmark achievement in this field is the report by Ishihara and co-workers of the first example of a highly enantioselective terpene halopolycyclization, employing chiral phosphoramidite promoters (Scheme 9a).<sup>25</sup> In the illustrated example, phosphoramidite 44 is converted into a chiral halogenating agent 45 upon treatment with *N*-iodosuccinimide, which enables enantioselective iodonium ion formation (46), and subsequent cationic cascade cyclization to tetracycle 47. Due to the formation of





Scheme 7 Oxidative epoxide-opening cyclization approach to lactodehydrothrysiferol (Florencig and co-workers).



Scheme 8 Nicholas reaction-triggered epoxide-opening cascade in the synthesis of teurilene (Martin and co-workers).

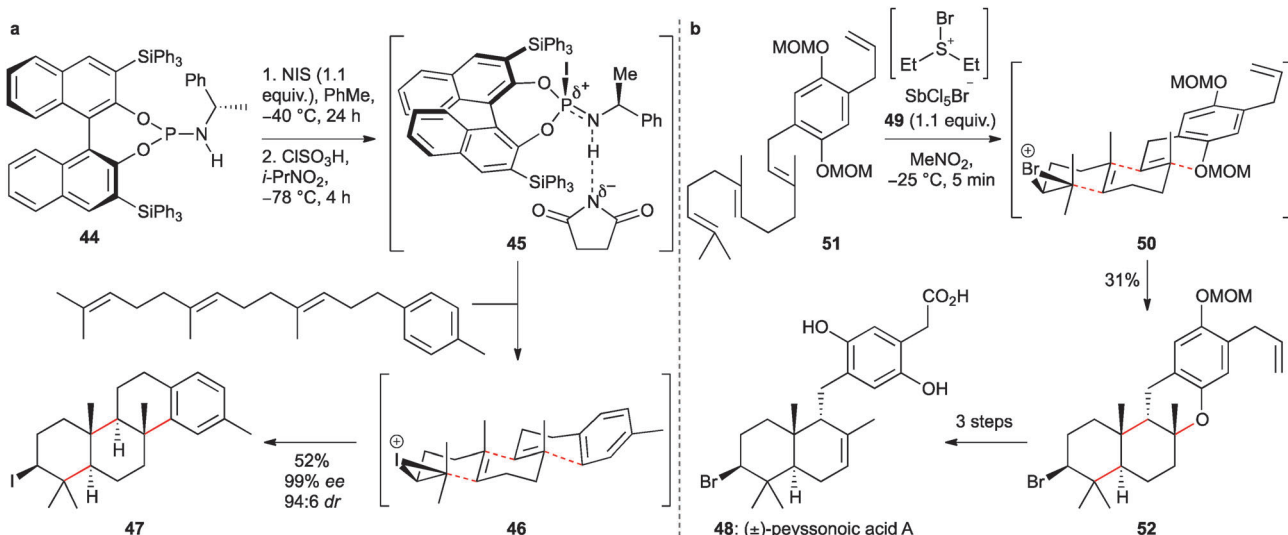
some monocyclic intermediates, exposure of the crude reaction mixture to chlorosulfuric acid ( $\text{ClSO}_3\text{H}$ ) ensures complete conversion to fully cyclized products, with **47** isolated in good yield (52%) and excellent stereoselectivity (99% ee, 94:6 dr). The use of a sterically hindered phosphoramidite and an apolar solvent (toluene) was crucial to the success of this chemistry: it was proposed that key complex **45** may exist as a tight ion pair, with a relatively strong hydrogen bond to the succinimide

ion restricting P–N bond rotation, thus enhancing the level of stereocontrol.

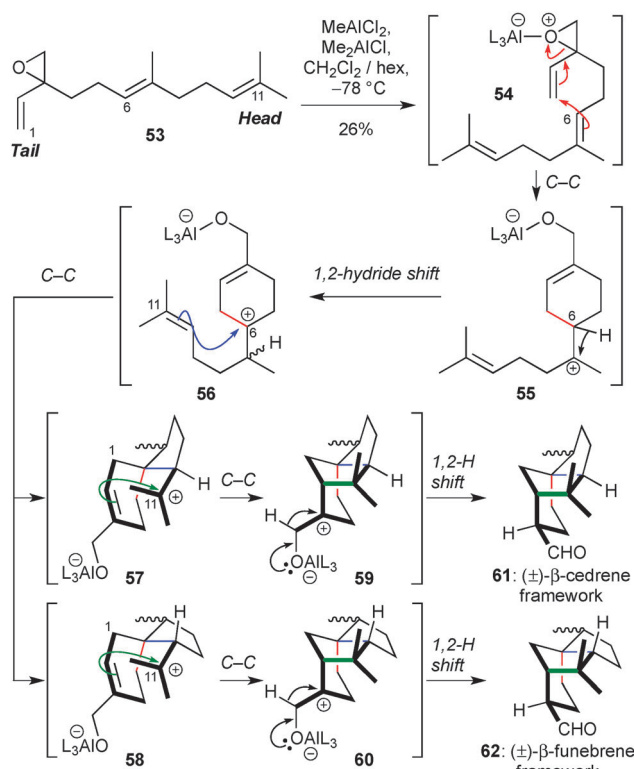
Snyder and co-workers' studies on polyene cyclizations induced *via* more elusive chloronium and bromonium ions have led to the synthesis of several natural products,<sup>26</sup> including ( $\pm$ )-peyssonnic acid A (**48** Scheme 9b). Being a marine natural product, a bromonium ion-initiated cyclization has clear biosynthetic relevance. However, a key design element for this reactivity is the need to inhibit the nucleophilicity and basicity of the counteranion, which could otherwise compete in the bromonium ion ring opening. This is achieved by the use of bromodiethylsulfonium bromopentachloroantimonate (**49**) to promote formation of bromonium ion **50** from polyene **51**, capture of which by the two alkenes and phenolic ether gives **52**. This cyclization, which builds three rings in a single operation, is only three steps from the natural product **48**.

Terpene cyclizations can be classified by the direction of charge propagation. Biomimetic total syntheses invariably employ head-to-tail (HT) cyclizations, in which the cation is formally transmitted from the branched 'head' of the terpene to the nucleophilic 'tail'. However, the total synthesis of the strained funebrene and cedrene natural products by Pronin and Shenvi (Scheme 10) illustrates an intriguing realization of the relatively unexplored tail-to-head (TH) cyclization mode.<sup>27</sup> The chemistry has many of the characteristics of a traditional HT approach – it involves a Lewis acid-promoted epoxide opening to promote cyclization – and also several Wagner–Meerwein rearrangements. However, key to the success of this work is sequestration of the Lewis acid counteranion at the tail end of the terpenoid, which is achieved through strong aluminium–heteroatom bonds. This separates the counterion from the developing cationic centres, and thus prevents undesirable elimination (E1) or cation–anion recombination processes.

Following complexation of epoxide **53** by the aluminium(III) Lewis acid, ring-opening at the allylic position leads to tertiary cyclohexylalkyl cation (**54**  $\rightarrow$  **55**), which undergoes a 1,2-hydride shift to afford cyclohexyl cation **56**. This cation is now appropriately disposed to undergo attack by the remaining alkanyl chain, a non-diastereoselective process that affords epimeric mixtures of the spirocyclic tertiary cations **57** and **58**. In both cases, the cation is positioned in proximity to the cyclohexene ring,



Scheme 9 Halonium ion-initiated polycyclizations (a Ishihara, b Snyder, and co-workers).

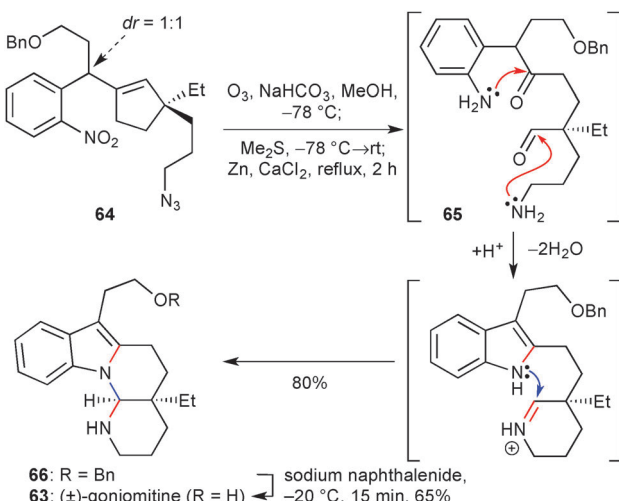
Scheme 10 Tail-to head biomimetic assembly of the  $\beta$ -cedrene and  $\beta$ -funebrene natural products (Pronin and Shenvi).

and through a final cyclization process affords cations **59** and **60**. The predominant final products **61** and **62** (the  $\beta$ -cedrene and  $\beta$ -funebrene skeletons) then arise from a 1,2-hydride shift driven by carbonyl formation. The lack of stereoselectivity in this reaction is interesting, and may in part arise from the enforced stepwise cyclization pathway in the TH manifold, compared to the chair-like conformations that are accessible in HT cyclizations.<sup>28</sup> The laboratory realization of these complex

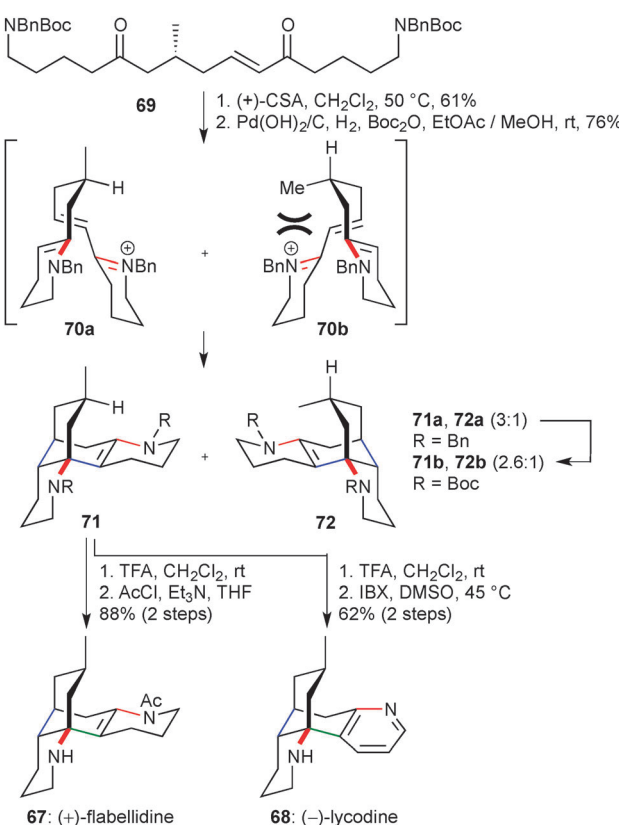
biosynthetic pathways is nonetheless an impressive and informative achievement.

The *Aspidosperma* alkaloids have long attracted the attention of synthetic chemists due to their bioactivities and fascinating diversity of structures, which offer many opportunities for cascade cyclizations.<sup>29</sup> In this context, Zhu and co-workers have recently developed a unified oxidation/reduction/cyclization sequence that constructs the polycyclic core of the cytotoxic *Aspidosperma* alkaloid ( $\pm$ )-goniomitine (**63**, Scheme 11) along with four other structurally related members of the family.<sup>30</sup> The one-pot cyclization commences with ozonolysis of **64** to generate a diketone, with an *in situ* zinc-mediated reduction of the nitro group and azide yielding the key diamine intermediate **65**. Under the moderately acidic reaction conditions, this triggers a double condensation, and then cyclization of the resulting indole nitrogen atom onto the pendent iminium ion with exclusive formation of a *cis*-fused ring junction. A Birch reduction is employed on compound **66** to effect debenzylation, which affords the natural product **63**.

The *Lycopodium* alkaloids (e.g. flabellidine **67**, and lycodine **68**, Scheme 12) have also been a subject of some interest, again by virtue of their biological activities and unique bicyclo[3.3.1]-nonane that are fused to two peripheral piperidine rings.<sup>31</sup> Takayama and co-workers have developed an impressive biomimetic tricyclization cascade to access these two natural products from a minimally functionalized, acyclic starting material **69**. The cyclization is initiated by deprotection of the two terminal amines in **69**, which spontaneously cyclize to give the enamine-iminium ion intermediate **70**. The diastereoselectivity of the ensuing Michael cyclization is proposed to be controlled by the single pre-installed stereogenic centre, where conformer **70b** is disfavoured by a steric clash between the pseudo-axial methyl group and the forming ring system, which is not present in conformer **70a**. The conjugated iminium ion formed from this Michael addition is then in turn trapped by the enamine of the other ring, leading (after further tautomerization) to tetracycle



Scheme 11 Oxidation/reduction/cyclization sequence towards (±)-goniomitine (Zhu and co-workers).



Scheme 12 Iminium ion/enamine biomimetic cascade route to (+)-flabellidine and (-)-lycodine (Takeyama and co-workers).

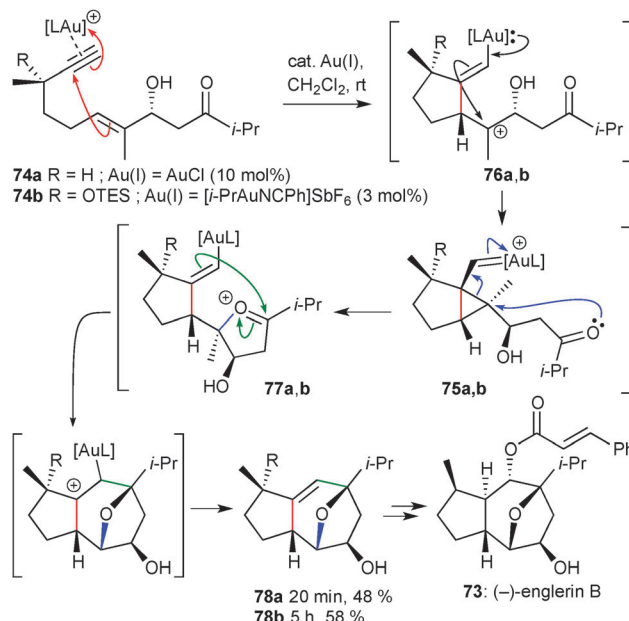
71a, and its diastereomer 72a (61%, 71a: 72a = 3:1). Separation of these compounds was most readily achieved by temporary functionalization of the amines as *tert*-butyl carbamates 71b and 72b; regioselective acetylation of 71b yielded (+)-flabellidine 67, or IBX-mediated oxidation furnished (-)-lycodine 68. This synthetic ideal was contemporaneously utilized by Smith and co-workers in a synthesis of the related natural product (-)-gephyrotoxin.<sup>32</sup>

## Metal-catalyzed cascades

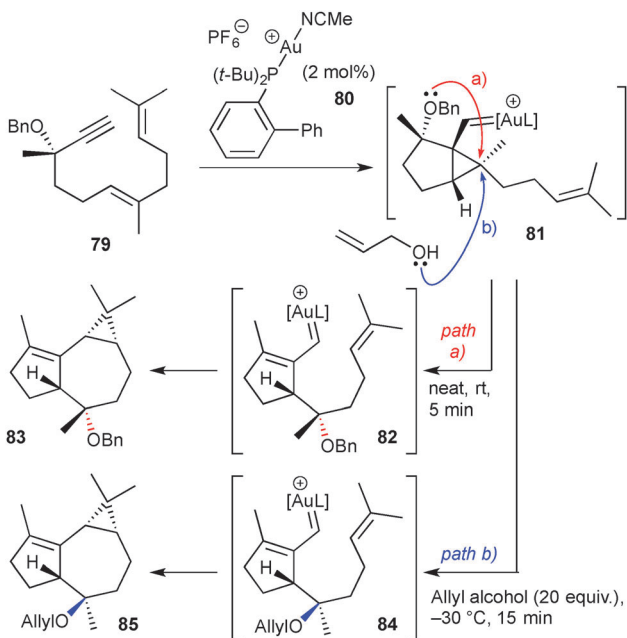
Metal-catalyzed reactions offer an exceptional means to engineer cascade processes, due to their high functional group tolerance, orthogonality to other reaction manifolds, and most importantly their ability to construct a wide variety of complex structures through unique but highly selective mechanistic pathways. In many cases, metal catalysis is synonymous with high atom economy,<sup>33</sup> particularly for cycloisomerization reactions,<sup>34</sup> where a number of applications in the synthesis of natural products have been reported in recent years.

The explosion of research in gold catalysis has inevitably led to some elegant synthetic demonstrations,<sup>35,36</sup> two examples have been selected which highlight the level of fine-tuned molecular complexity that can be achieved with this metal. The first involves two syntheses of the sesquiterpene (-)-englerin B (73, Scheme 13) reported concurrently by the Echavarren<sup>37</sup> and Ma groups.<sup>38</sup> These syntheses vary only in the nature of the propargylic substituent in enyne 74, which leads to different synthetic endgames. These cascades initiate by complexation of the alkyne in 74 to the gold(i) cation, which triggers cyclopropane formation (75) *via* alkynylgold species 76. Nucleophilic ring opening of the cyclopropane by the carbonyl leads to oxocarbenium ion 77; a deaurative Prins-type cyclization completes the tricyclic core 78 of englerin B.

Following this work, the Echavarren group published syntheses of three aromadendrane natural products (Scheme 14).<sup>39</sup> This more recent report is noteworthy for the exquisite control over the stereochemical outcome of the gold-catalyzed cascade that is achieved by simple but logical variation of the reaction conditions. Thus, reaction of dienyne 79 with catalyst 80 (neat) leads, *via* carbенoid 81, to an intramolecular transfer of the benzyloxy group to give carbенoid 82 (path a), and then tricycle 83,



Scheme 13 Gold-catalyzed cascades towards (-)-englerin B (series a: Ma and co-workers; series b: Echavarren and co-workers).

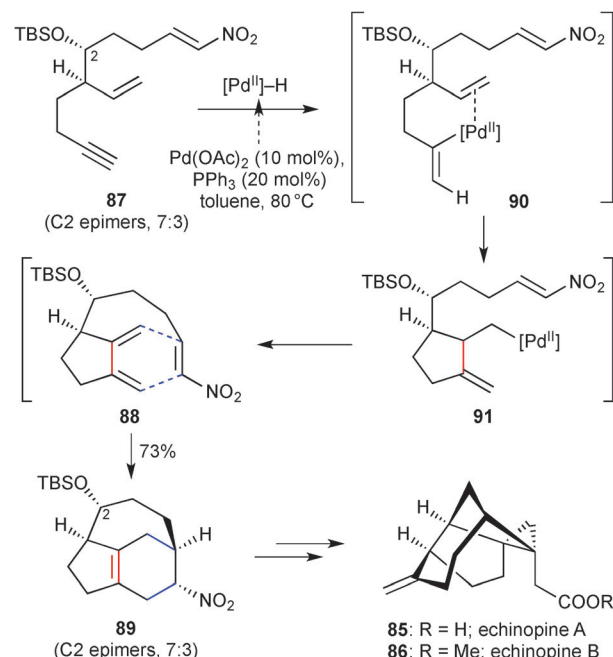


Scheme 14 Nucleophile-tuned approach to three aromadendrane natural products (Echavarren and co-workers).

a precursor to  $(-)$ -4 $\beta$ ,7 $\alpha$ -aromadendranediol and  $(-)$ -epiglobulol. Alternatively, equivalent reaction in the presence of an excess of allyl alcohol results in intermolecular ring-opening of 81 to the epimeric carbenoid 84/tricyclic 85 (path b), *en route* to  $(-)$ -4 $\alpha$ ,7 $\alpha$ -aromadendranediol.

The formal syntheses of echinopines A and B (85 and 86, Scheme 15) by Chen and co-workers<sup>40</sup> highlights the potential of palladium-catalyzed cycloisomerization<sup>41</sup> to construct dienes that are suitable for subsequent Diels–Alder cycloadditions. Treatment of the acyclic dienyne 87 with palladium(II) acetate/triphenylphosphine in toluene at  $80^\circ\text{C}$  leads to the formation of diene 88, which undergoes *in situ* cycloaddition with the pendent nitroalkene to form tricyclic product 89 in 73% yield – an impressive increase in molecular complexity *via* a highly atom-economical process. The mechanism of this cycloisomerization remains somewhat unclear; one possibility<sup>41</sup> is the initial generation of a palladium(II) hydride species, which mediates the cyclization by alkyne hydropalladation (90), then migratory insertion of the proximal alkene (91), and finally  $\beta$ -hydride elimination to deliver the 1,3-diene product. The 7:3 mixture of epimers at the C2 position is inconsequential, as this oxygen substituent is destined for conversion to an exocyclic alkene in the natural products.

Carbopalladation cascades<sup>42</sup> represent an enabling and readily implemented method to achieve polycyclizations. Two examples that epitomize the level of synthetic challenge that can be conquered with this chemistry are shown in Scheme 16. The first, a synthesis of linoexpin (92, Scheme 16a) reported by the Tietze group,<sup>43</sup> involves domino cyclization of an aryl bromide 93 onto an alkyne, with capture of intermediate alkenylpalladium species 94 by an appended allylsilane, which gives a high yield of the pentacyclic product 95. The allylsilane is crucial in controlling the positioning of the exocyclic alkene in 95; among several

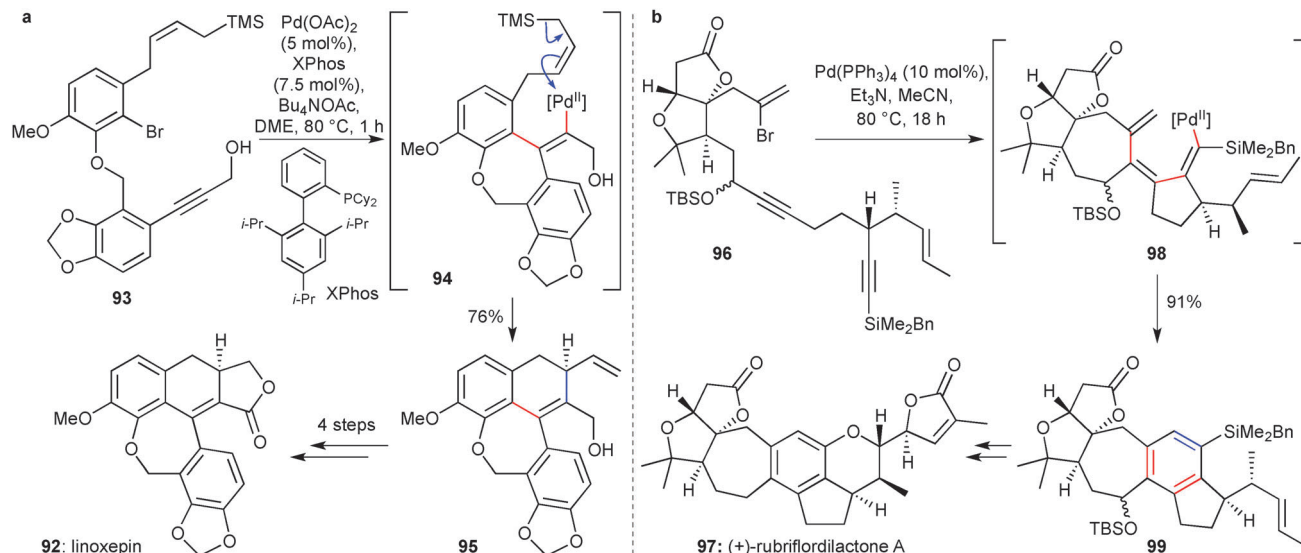


Scheme 15 Cycloisomerization/Diels–Alder approach to echinopines A and B (Chen and co-workers).

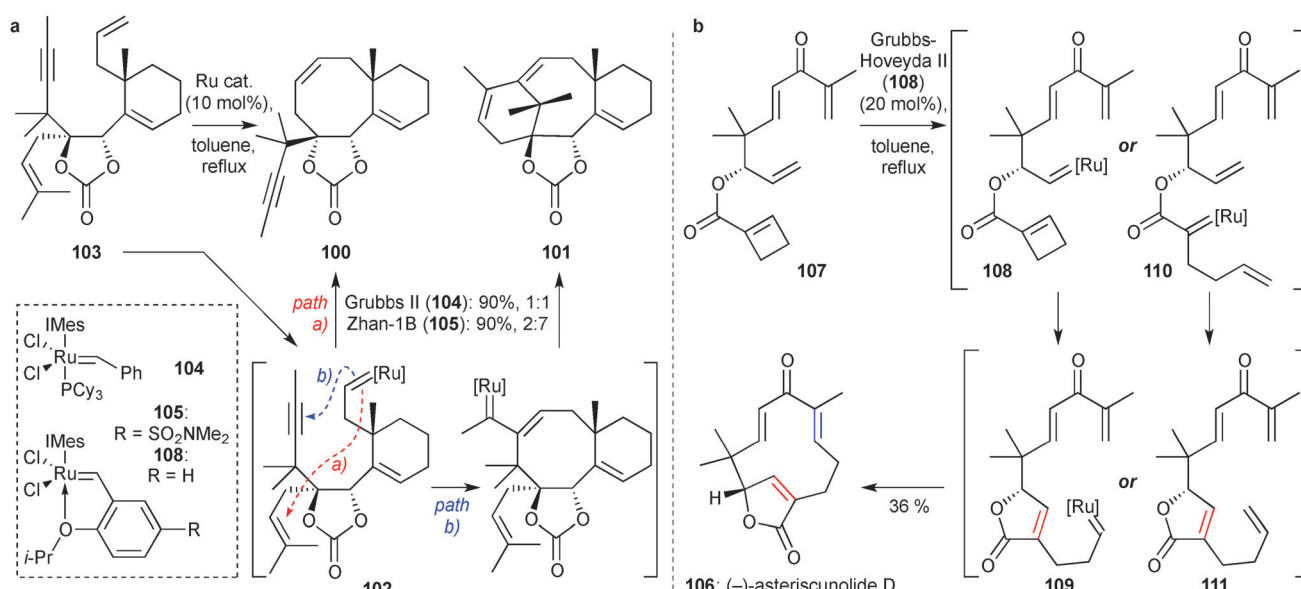
mechanisms that could be envisaged for this final step, this may suggest a desilylative palladation of 94 (perhaps proceeding *via* a silicon-stabilized carbocation), prior to rapid reductive elimination; or alkene carbopalladation, followed by an unusual formal  $\beta$ -silyl elimination. The second example depicts the cascade cyclization of a complex bromoendiyne 96, used to construct the 7,6,5-tricyclic core of rubriflordilactone A (97) in a total synthesis of this natural product by the Anderson group (Scheme 16b).<sup>44</sup> A sequence of two carbopalladations leads to intermediate trienyl-palladium complex 98; 6 $\pi$ -electrocyclization/ $\beta$ -hydride elimination, or alkene electrophilic palladation/reductive elimination, are possible mechanisms that could be envisaged to complete the cyclization of 98 to pentacycle 99. This product was advanced to rubriflordilactone A in a further 6 steps.

Metathesis reactions remain a productive source of highly atom-efficient cascade polycyclizations. In this context, Prunet and co-workers have achieved an enantioselective synthesis of the ABC tricyclic core of Taxol *via* a cascade ene–yne–ene RCM reaction (Scheme 17a).<sup>45</sup> This application is particularly notable due to the inherent ring strain and complexity of the Taxol system, which still presents one of the most imposing challenges to synthetic chemists. Here, this challenge is epitomized by the problematic formation of an ene–ene RCM byproduct 100 (path a) along with the desired ene–yne–ene product 101 (path b), depending on which unsaturated component the ruthenium carbene (102, formed on initial metathesis with the unhindered terminal alkene in 103) engages with. This product selectivity shows high catalyst dependence: where the Grubbs II catalyst 104 gives a high yield but equimolar ratio of 100 and 101, the Zhan 1B variant 105 is much more selective for the desired product 101.





Scheme 16 Carbopalladation cascades in the synthesis of linoxepin (a, Tietze and co-workers) and (+)-rubriflordilactone A (b, Anderson and co-workers).



Scheme 17 Metathesis cascades in the synthesis of the Taxol ABC ring system (a, Prunet and co-workers), and (-)-asteriscunolide D (b, Li and co-workers).

Another impressive ruthenium-catalyzed metathesis cascade has been reported by the Li group,<sup>46</sup> in which a divergent synthesis of several humulanolide natural products is realized. These anticancer targets, exemplified by (-)-asteriscunolide D (106, Scheme 17b), comprise a challenging 11-membered ring core featuring an *ansa*-butenolide unit. The highly creative approach employed by the Li group harnesses the ring strain of a cyclobutene to control formation of these two rings. Two possible mechanisms are shown, with the catalyst having a choice of initiation sites at the unhindered terminal alkene in 107, or the strained (but electron-deficient) cyclobutene. The authors propose the former pathway, with a subsequent strain

release-driven ring-opening metathesis (ROM) reaction of the cyclobutene 108 leading to the butenolide unit 109, with the ruthenium carbenoid transferred to the ring-opened side chain. This then undergoes RCM with the 1,1-disubstituted alkene, affording (-)-asteriscunolide D (36% yield). Alternatively, initial reaction through cyclobutene ring opening (110), and metathesis with the terminal alkene, could afford intermediate 111 prior to a separate ring-closing macrocyclization. Either way, the formation of an 11-membered macrocycle through this cascade is an impressive achievement, and the value of this chemistry is further enhanced through transformation of asteriscunolide D into several other natural products.

A highlight in transition metal-catalyzed polycyclization is the recent development of pseudo-biomimetic enantioselective polyene cyclizations,<sup>47</sup> albeit applications in natural product synthesis remain rare. The Carreira group's realization of iridium-catalyzed asymmetric polyene cyclization is therefore highly significant, depicted in Scheme 18a in the context of a biosynthetic approach to the labdane diterpene (+)-asperolide C, **112**.<sup>48</sup> Building on previous methodology in which electron-rich arenes terminate the cationic cascade,<sup>49</sup> an allyl silane is here employed as the terminating group. Thus, generation of a chiral  $\pi$ -allyl iridium complex **113** from allylic acetate **114** initiates a cascade of stereoselective cyclizations before final loss of this TMS group, forming the *trans*-decalin **116** with excellent stereocontrol (96% ee, 9:1 dr). This tricyclic scaffold was taken on to (+)-asperolide C (**112**) in a further ten steps.

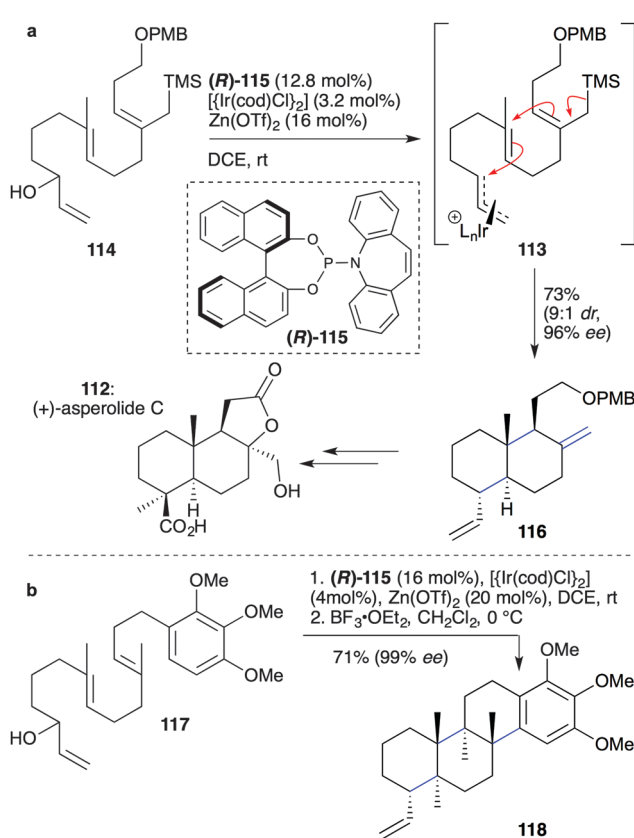
This chemistry has significant potential as a general method for the synthesis of terpene natural products, as recognized by the Li group in an impressive synthesis of mycoleptodiscin A, where three rings are formed in a single step (Scheme 18b).<sup>50</sup> Under the cyclization conditions,<sup>49</sup> polyene **117** gave the product **118**, albeit in low yield (21%). However, side products arising from premature termination of the cascade could be encouraged to undergo further stereoselective cyclization on treatment with  $\text{BF}_3\text{-OEt}_2$ , achieving an overall yield of 71% for this sequence, with exceptionally high enantioselectivity (> 99% ee). That these

interrupted cascade products were also formed in high enantio-purity implies, as proposed by Carreira,<sup>49</sup> that the catalyst exerts stereocontrol over the first cyclization step only; the stereochemistry locked into the first formed ring then acts to direct the subsequent cascade with exquisite control.

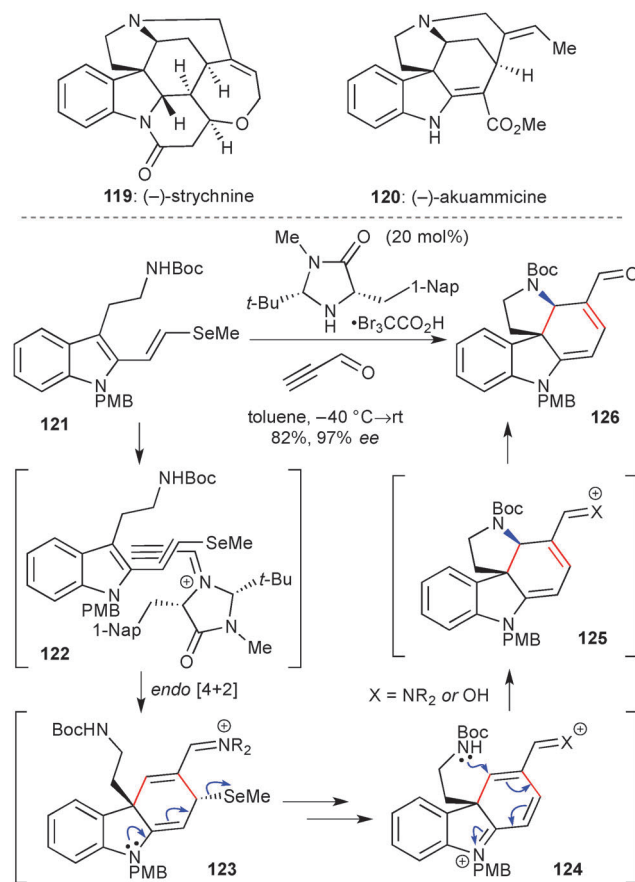
## Organocatalytic cascades

Efficiency in Nature is often enhanced by the formation of multiple natural products from a common biosynthetic intermediate. This is also a tantalizing goal in chemical synthesis, and as such it is perhaps surprising that asymmetric organocatalysis has yet to be widely exploited in this diversifying context. Nonetheless, this is an ideal embraced in the MacMillan group's 'collective' total synthesis of six indole alkaloids, including strychnine (**119**, Scheme 19) and akuammicine (**120**).<sup>51</sup> All are accessed from a single form of advanced intermediate, prepared with high enantio- and diastereoselectivity *via* an organocascade polycyclization.

This cascade begins with an *endo*-selective Diels–Alder reaction between 2-(vinyl-1-selenomethyl)tryptamine **121** and propynal, with enantioselectivity deriving from orientation of the alkyne of the imidazolium ion (**122**) away from the bulky *tert*-butyl group, and an enforced approach of the selenyl diene to the top



Scheme 18 Enantioselective iridium-catalyzed polyene cyclizations in the synthesis of (+)-asperolide C (a, Carreira and co-workers) and mycoleptodiscin A (b, Li and co-workers).



Scheme 19 Collective total synthesis of *Strychnos* alkaloids using an organocatalytic cascade (MacMillan and co-workers).



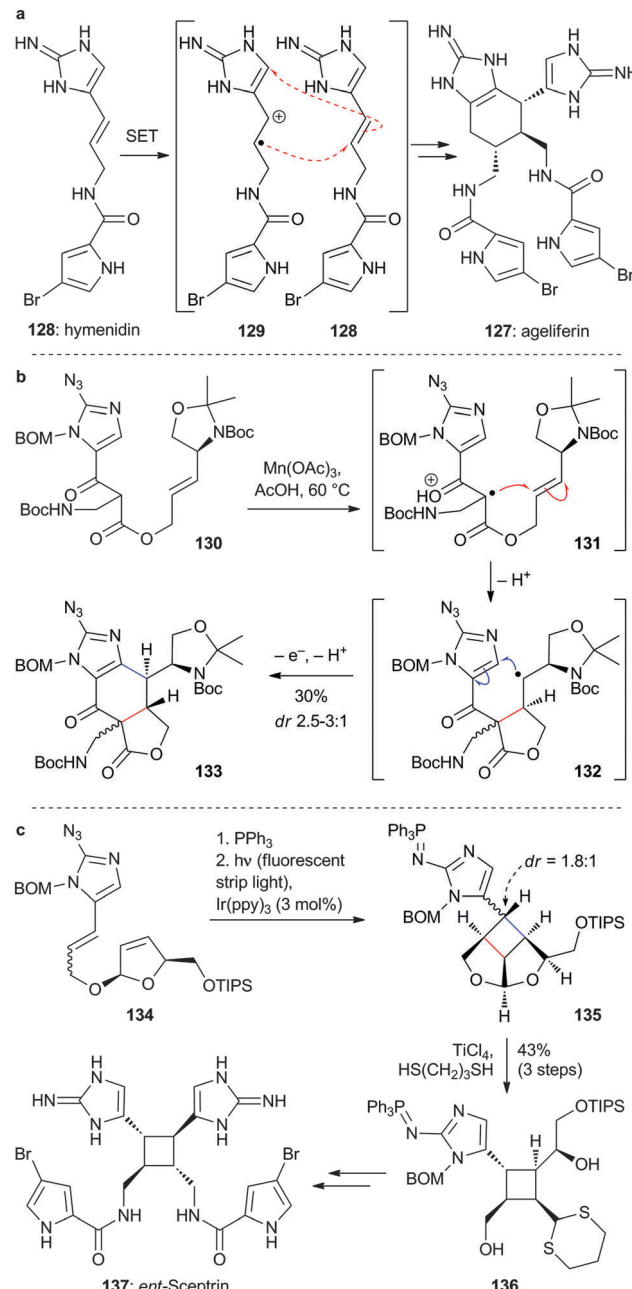
face as illustrated (where the naphthyl group blocks the lower face of the reacting alkyne). The choice of a selenyl substituent is key in enabling its subsequent  $\beta$ -elimination from 123, affording iminium ion 124. The pendent sidechain carbamate nitrogen atom then performs a 5-*exo*-trig cyclization to form intermediate 125, before or after hydrolytic recycling of the catalyst. 126 was transformed into akuammicine in a further six steps, and into strychnine in a further eight steps; with a total count of twelve steps and an overall yield of 6.4%, this is the shortest enantioselective route strychnine completed to date: a level of efficiency that is possible solely through the use of the cascade strategy. Simple variation of the nitrogen protecting group enabled the synthesis of four other indole alkaloids.

## Radical cascades

Recent applications of radical chemistry in polycyclizations have seen use of classical methods (*e.g.* manganese(III) acetate) and emerging technologies (*e.g.* photoredox catalysis) to mediate radical pathways. Both have been elegantly demonstrated in the extensive work of the Chen group on the synthesis of the pyrrole-imidazole alkaloids ageliferin, sceptrin and massadine. Whilst only two new rings are produced in the course of this cascade process, these groundbreaking examples pave the way for more ambitious applications. As in the incarvitolone/incarvilleatone natural products mentioned earlier in this review, these sponge metabolites derive from dimerization of simpler natural products, in this instance through formal [4+2], [3+2], and [2+2] cycloadditions of oroidin and its derivatives.<sup>52</sup> This relationship makes a common synthetic approach to these compounds an attractive prospect. The biosynthesis of ageliferin (127, Scheme 20a) provides an informative backdrop to this synthetic chemistry: enzymatic single electron transfer (SET) oxidation of the monomer hymenidin (128) leads to radical cation 129, which reacts with another molecule of hymenidin 128. The subsequently formed radical has a choice of positions to effect ring closure (thus leading to different natural products); in the case of ageliferin it is a 6-membered ring that forms, giving the natural product after further SET and tautomerization.

An oxidative radical cyclization was designed by the Chen group to mimic this biosynthetic dimerization (Scheme 20b). Manganese(III) acetate-promoted oxidation of  $\beta$ -ketoester 130 gives radical cation 131, which undergoes a 5-*exo*-trig cyclization onto the pendent olefin to give radical 132. This in turn then engages in a 6-*endo*-trig cyclization onto the imidazole ring, a cyclization that is neatly promoted over the competing 5-*exo* process by the driving force of captodative stabilization of the resultant radical. Further SET oxidation and deprotonation affords product 133, which was taken on to ageliferin, bromogeliferin, and dibromoageliferin.<sup>53</sup>

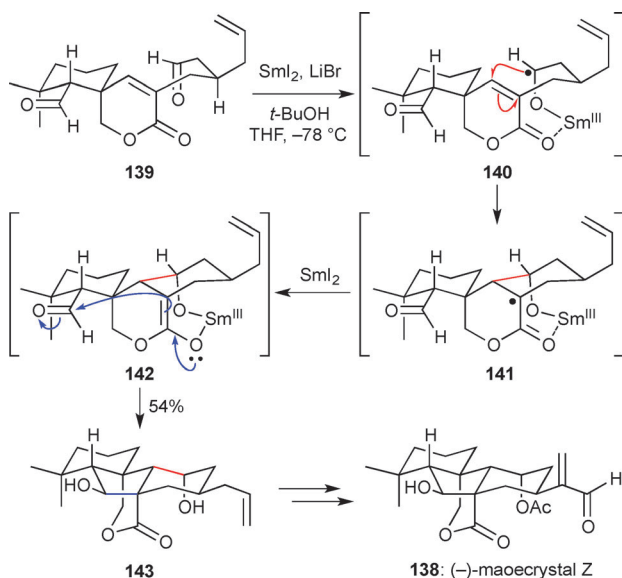
The Chen group has also accomplished enantioselective syntheses of the sceptrin natural products, again using biomimetic oxidative cyclizations.<sup>50</sup> In this case, the key cascade cyclization of substrate 134 was attempted with several single electron oxidants, but success was only met *via* a photoredox strategy involving



Scheme 20 Synthesis of pyrrole-imidazole natural products by radical cascades (Chen and co-workers).

reversible single electron transfer between the substrate (the amino-imidazole group) and  $\text{Ir}(\text{ppy})_3$  catalyst (Scheme 20c). This imaginative chemistry gave cyclization product 135 (1.8 : 1 dr), with the sceptrin core 136 revealed through exposure of 135 to titanium tetrachloride and 1,3-propanedithiol. This cyclobutane was taken on to complete the synthesis of *ent*-sceptrin (137); these enantioselective syntheses in fact led to a call for a reassignment of the absolute stereochemistry of both sceptrin and ageliferin, as each led to the unanticipated antipode of the natural products. This has raised the interesting concept of 'enantiodivergent biosynthesis' (see also Scheme 6), in which





Scheme 21  $\text{SmI}_2$ -mediated cascade cyclization in the synthesis of  $(-)$ -maoecrystal Z (Reisman and co-workers).

opposite pseudo-enantiomeric series of natural products are produced by monomer homo/heterodimerization, with the oxidative dimerization processes being mediated by discrete enzymes, rather than a common biosynthetic pathway as had been assumed prior to this work.

Samarium(II) iodide chemistry has experienced a renaissance in recent years, not least through the realization of some ambitious, complexity-inducing transformations mediated by this reagent.<sup>54</sup> A recent example that highlights the utility of this chemistry is found in a synthesis of maoecrystal Z (138, Scheme 21) by the Reisman group.<sup>55</sup> Containing six contiguous stereocentres within a congested tetracyclic ring system, this molecule clearly represents a significant synthetic challenge.

The key radical cascade was deployed at a relatively late stage of the synthesis. Model studies had revealed the beneficial effect of performing the  $\text{SmI}_2$ -mediated reductive cyclization in the presence of a lithium halide and *t*-BuOH, where the lithium salt is believed to increase the reducing power of the samarium diiodide, while the alcohol acts as a proton source. Application of these conditions to dialdehyde 139 initially leads to ketyl radical anion generation at the least sterically-hindered aldehyde (140). This is followed by cyclization to 141, with a further single-electron reduction forming enolate 142, which engages in intramolecular aldol cyclization onto the remaining aldehyde to give tetracycle 143 in a remarkable 54% yield as a single diastereomer. The high stereoselectivity of the radical cyclization was rationalised by orientation of the aldehyde such that destabilizing steric interactions with the proximal cyclohexane ring are minimized; chelation of the samarium to the lactone carbonyl may also be of importance. The stereoselectivity of the final aldol cyclization is likely controlled by a pseudo-equatorial positioning of the aldehyde. 143 was taken on to complete the first total synthesis of  $(-)$ -maoecrystal Z, with just 12 steps in the longest linear sequence.

## Conclusions

Emerging technologies inspire the design of ambitious yet functional group tolerant cascade approaches to natural products. It seems inevitable that new methods (such as dual catalysis, organocatalysis, and photoredox catalysis) will find increasing use in the natural product arena. Challenges yet remain: for example, the design and implementation of truly flexible total synthetic routes would enhance the implementation of natural products – and analogues – in medicinal chemistry; the efficiency imparted by cascade cyclizations could well be vital to such endeavours. The field of natural product synthesis thus stands at a crossroads, where synthetic ingenuity can finally access complex architectures with genuine, scalable efficiency. Wherever the field moves over the next decade, it will surely continue to excite and capture the imagination of organic chemists.

## Acknowledgements

RA, DFJC, SMM, HS, YX are supported by the EPSRC Centre for Doctoral Training in Synthesis for Biology and Medicine (EP/L015838/1). RA also thanks the Development and Promotion of Science and Technology Talents Project (DPST), Royal Thai Government for a scholarship. SMM also thanks the Oxford-Radcliffe fund for a scholarship. YX also thanks the University of Oxford Clarendon fund for a scholarship. EAA thanks the EPSRC for support (EP/M019195/1).

## Notes and references

1. A. Bauer and M. Bronstrup, *Nat. Prod. Rep.*, 2014, **31**, 35–60.
2. A. L. Harvey, R. Edrada-Ebel and R. J. Quinn, *Nat. Rev. Drug Discovery*, 2015, **14**, 111–129.
3. M. S. Butler, A. A. B. Robertson and M. A. Cooper, *Nat. Prod. Rep.*, 2014, **31**, 1612–1661.
4. K. C. Nicolaou and J. S. Chen, *Chem. Soc. Rev.*, 2009, **38**, 2993–3009.
5. E. A. Anderson, *Org. Biomol. Chem.*, 2011, **9**, 3997–4006.
6. *Domino Reactions: Concepts for Efficient Organic Synthesis*, ed. L. F. Tietze, Wiley-VCH, Weinheim, 2014.
7. M. Razzak and J. K. De Brabander, *Nat. Chem. Biol.*, 2011, **7**, 865–875.
8. C. M. Beaudry, J. P. Malerich and D. Trauner, *Chem. Rev.*, 2005, **105**, 4757–4778.
9. R. Webster, B. Gaspar, P. Mayer and D. Trauner, *Org. Lett.*, 2013, **15**, 1866–1869.
10. C. Yuan, B. Du, L. Yang and B. Liu, *J. Am. Chem. Soc.*, 2013, **135**, 9291–9294.
11. B. Du, C. Yuan, T. Yu, L. Yang, Y. Yang, B. Liu and S. Qin, *Chem. – Eur. J.*, 2014, **20**, 2613–2622.
12. T. Kang, S. B. Song, W.-Y. Kim, B. G. Kim and H.-Y. Lee, *J. Am. Chem. Soc.*, 2014, **136**, 10274–10276.
13. C. W. Plummer, C. S. Wei, C. E. Yozwiak, A. Soheili, S. O. Smithback and J. L. Leighton, *J. Am. Chem. Soc.*, 2014, **136**, 9878–9881.



14 A. C. Jones, J. A. May, R. Sarpong and B. M. Stoltz, *Angew. Chem., Int. Ed.*, 2014, **53**, 2556–2591.

15 Y. Sawayama and T. Nishikawa, *Angew. Chem., Int. Ed.*, 2011, **50**, 7176–7178.

16 P. D. Brown, A. C. Willis, M. S. Sherburn and A. L. Lawrence, *Org. Lett.*, 2012, **14**, 4537–4539.

17 I. Vilotijevic and T. F. Jamison, *Angew. Chem., Int. Ed.*, 2009, **48**, 5250–5281.

18 C. J. Morten, J. A. Byers, A. R. Van Dyke, I. Vilotijevic and T. F. Jamison, *Chem. Soc. Rev.*, 2009, **38**, 3175–3192.

19 Y. Zhu, Q. Wang, R. G. Cornwall and Y. Shi, *Chem. Rev.*, 2014, **114**, 8199–8256.

20 D. J. Clausen, S. Wan and P. E. Floreancig, *Angew. Chem., Int. Ed.*, 2011, **50**, 5178–5181.

21 S. Wan, H. Gunaydin, K. N. Houk and P. E. Floreancig, *J. Am. Chem. Soc.*, 2007, **129**, 7915–7923.

22 V. S. Kumar, D. L. Aubele and P. E. Floreancig, *Org. Lett.*, 2001, **3**, 4123–4125.

23 J. Rodríguez-López, F. Pinacho Crisóstomo, N. Ortega, M. López-Rodríguez, V. S. Martín and T. Martín, *Angew. Chem., Int. Ed.*, 2013, **52**, 3659–3662.

24 D. D. Diaz, J. M. Betancort and V. S. Martin, *Synlett*, 2007, 343–359.

25 A. Sakakura, A. Ukai and K. Ishihara, *Nature*, 2007, **445**, 900–903.

26 S. A. Snyder, D. S. Treitler and A. P. Brucks, *J. Am. Chem. Soc.*, 2010, **132**, 14303–14314.

27 S. V. Pronin and R. A. Shenvi, *Nat. Chem.*, 2012, **4**, 915–920.

28 R. A. Shenvi and E. J. Corey, *Org. Lett.*, 2010, **12**, 3548–3551.

29 Z. R. Xu, Q. Wang and J. P. Zhu, *J. Am. Chem. Soc.*, 2013, **135**, 19127–19130.

30 O. Wagnieres, Z. R. Xu, Q. Wang and J. P. Zhu, *J. Am. Chem. Soc.*, 2014, **136**, 15102–15108.

31 M. Azuma, T. Yoshikawa, N. Kogure, M. Kitajima and H. Takayama, *J. Am. Chem. Soc.*, 2014, **136**, 11618–11621.

32 S. Y. Chu, S. Wallace and M. D. Smith, *Angew. Chem., Int. Ed.*, 2014, **53**, 13826–13829.

33 B. M. Trost, *Science*, 1991, **254**, 1471–1477.

34 V. Michelet, P. Y. Toullec and J. P. Genet, *Angew. Chem., Int. Ed.*, 2008, **47**, 4268–4315.

35 A. S. K. Hashmi and M. Rudolph, *Chem. Soc. Rev.*, 2008, **37**, 1766–1775.

36 M. Rudolph and A. S. K. Hashmi, *Chem. Soc. Rev.*, 2012, **41**, 2448–2462.

37 K. Molawi, N. Delpont and A. M. Echavarren, *Angew. Chem., Int. Ed.*, 2010, **49**, 3517–3519.

38 Q. Zhou, X. Chen and D. Ma, *Angew. Chem., Int. Ed.*, 2010, **49**, 3513–3516.

39 J. Carreras, M. Livendahl, P. R. McGonigal and A. M. Echavarren, *Angew. Chem., Int. Ed.*, 2014, **53**, 4896–4899.

40 P. A. Peixoto, R. Severin, C.-C. Tseng and D. Y. K. Chen, *Angew. Chem., Int. Ed.*, 2011, **50**, 3013–3016.

41 B. M. Trost, D. L. Romero and F. Rise, *J. Am. Chem. Soc.*, 1994, **116**, 4268–4278.

42 T. Vlaar, E. Ruijter and R. V. A. Orru, *Adv. Synth. Catal.*, 2011, **353**, 809–841.

43 L. F. Tietze, S.-C. Duefert, J. Clerc, M. Bischoff, C. Maaß and D. Stalke, *Angew. Chem., Int. Ed.*, 2013, **52**, 3191–3194.

44 S. S. Goh, G. Chaubet, B. Gockel, M.-C. A. Cordonnier, H. Baars, A. W. Phillips and E. A. Anderson, *Angew. Chem., Int. Ed.*, 2015, **54**, 12618–12621.

45 A. Letort, R. Aouzal, C. Ma, D.-L. Long and J. Prunet, *Org. Lett.*, 2014, **16**, 3300–3303.

46 J.-c. Han, F. Li and C.-c. Li, *J. Am. Chem. Soc.*, 2014, **136**, 13610–13613.

47 S. G. Sethofer, T. Mayer and F. D. Toste, *J. Am. Chem. Soc.*, 2010, **132**, 8276–8277.

48 O. F. Jeker, A. G. Kravina and E. M. Carreira, *Angew. Chem., Int. Ed.*, 2013, **52**, 12166–12169.

49 M. A. Schafroth, D. Sarlah, S. Krautwald and E. M. Carreira, *J. Am. Chem. Soc.*, 2012, **134**, 20276–20278.

50 S. Zhou, H. Chen, Y. Luo, W. Zhang and A. Li, *Angew. Chem., Int. Ed.*, 2015, **54**, 6878–6882.

51 S. B. Jones, B. Simmons, A. Mastracchio and D. W. C. MacMillan, *Nature*, 2011, **475**, 183–188.

52 Z. Ma, X. Wang, X. Wang, R. A. Rodriguez, C. E. Moore, S. Gao, X. Tan, Y. Ma, A. L. Rheingold, P. S. Baran and C. Chen, *Science*, 2014, **346**, 219–224.

53 X. Wang, X. Wang, X. Tan, J. Lu, K. W. Cormier, Z. Ma and C. Chen, *J. Am. Chem. Soc.*, 2012, **134**, 18834–18842.

54 M. Szostak, N. J. Fazakerley, D. Parmar and D. J. Procter, *Chem. Rev.*, 2014, **114**, 5959–6039.

55 J. Y. Cha, J. T. S. Yeoman and S. E. Reisman, *J. Am. Chem. Soc.*, 2011, **133**, 14964–14967.

